

PAPER • OPEN ACCESS

Theoretical and experimental investigations on a 12 kW Oxford-type dual-opposed moving-coil linear compressor

To cite this article: Jun Tan *et al* 2019 *IOP Conf. Ser.: Mater. Sci. Eng.* **502** 012039

View the [article online](#) for updates and enhancements.

Theoretical and experimental investigations on a 12 kW Oxford-type dual-opposed moving-coil linear compressor

Jun Tan^{1,3*}, Jiaqi Li^{1,2}, Rui Zha^{1,2}, Tao Zhang^{1,2}, Dingli Bao^{1,2}, Haizheng Dang^{1,3*}

¹State Key Laboratory of Infrared Physics, Shanghai Institute of Technical Physics, Chinese Academy of Sciences, 500 Yutian Road, Shanghai 200083, China

²University of Chinese Academy of Sciences, No.19A Yuquan Road, Beijing 100049, China

³Shanghai Boreas Cryogenics Co., Ltd, 1388 Shuidian Road, Shanghai 200434, China

*Corresponding author. Email: juntan@mail.sitp.ac.cn;
haizheng.dang@mail.sitp.ac.cn (Haizheng Dang)

Abstract. This paper presents theoretical and experimental investigations on an Oxford-type dual-opposed moving-coil linear compressor aiming to achieve an electric input power capacity of 12 kW, which is a great challenge in the moving-coil compressor field. A linearized model is established in which systematic analyses about force balance, mechanical resonance and magnetic circuit are conducted. The relations between air gap and magnetic field intensity in the magnetic circuit are focused on to optimize the motor efficiency, and the design of linear motor and mechanical spring are discussed in a more detailed way. The prototype compressor is worked out and tested, and experimental results are compared with theoretical analyses. The developed compressor will be coupled with a coaxial pulse tube cold head, which is expected to provide 600 W of cooling power at 77 K for cooling the high temperature superconducting (HTS) cables.

1. Introduction

Since the major breakthrough of high temperature superconducting (HTS) material in 1987, progress in relevant research has advanced considerably and many applications are foreseen for HTS technology, especially in the fields of electric and electronics. For instance, the HTS cable offers an excellent solution to the problem that the infrastructure must be improved to achieve high delivery efficiency of electric power, especially in long distance transportation, as the increased demand for electricity strains the capacity of electric grids around the worldwide. Superconducting components require reliable, low-cost, low-vibration sources of refrigeration. Otherwise, the cost of the added refrigeration system will be higher than the value of the saved energy, which does not make sense to improve the power grid infrastructure. Several types of cryocooler are currently available for HTS technology and have successfully implemented interfaces [1, 2]. As to the cooling of HTS cable in practical applications, not only the cooling capacity and efficiency but also the cryocooler vibration, mean time to fail and electromagnetic interference should be considered.



Due to the absence of moving component in the cold part, pulse tube cryocooler (PTC) has obvious advantages over other regenerative cryocoolers in term of lifetime, making it one of the most expected cryocoolers for cooling the HTS devices. Especially the Stirling-type PTC (SPTC), using the Oxford-type linear compressor as driving source, owing the advantages of small size and weight, low vibration and EMI, high reliability and long lifetime, has been applied into many practical HTS cable programs [3, 4].

The Oxford-type linear compressor, which owns advanced technics of flexure spring and clearance seal, the wear-out and lubrication are eliminated and both contamination and mechanic friction are substantially reduced compared with the conventional ones (such as the crank-shaft type, scroll type, etc.), thus is endowed with the merits of higher efficiency, stability and more compact structure. Nowadays, most of studies are mainly focused on small-capacity linear compressors with input power capacity below 1 kW (tens of or hundreds of watts). While for large ones (with input power capacity of several kilowatts or tens of kilowatts), relevant investigations have seldom been carried out and reported. In the cooling of HTS cables, a cooling power with hundreds or thousands watts at liquid nitrogen temperature is always needed. To improve this circumstance and prompt the development and application of SPTC in HTS industry, there is an urgent need to carry out investigations on large-capacity linear compressor. In this paper, theoretical and experimental investigations (including analyses of force balance, mechanical resonance, magnet circuit and detailed design) on a 12 kW dual-opposed Oxford-type moving-coil linear compressor are carried out, and a prototype compressor is worked out and tested.

2. Theoretical analyses

Fig. 1 shows the structure of the Oxford-type dual-opposed moving-coil linear compressor to be developed. The dual-opposed configuration is employed which can substantially decrease the fundamental frequency vibration. Each half includes a linear motor, a piston, two sets of flexure springs and several support components. During the operation, the piston, the coil and flexure springs will oscillate and the clearance seal acts as the dynamic seal between the piston and cylinder, thereby eliminating the source of rubbing wear and providing high reliability which is benefit for achieving long operation lifetime. The two halves share the same compression chamber and the PV power will be transported to the cold finger.

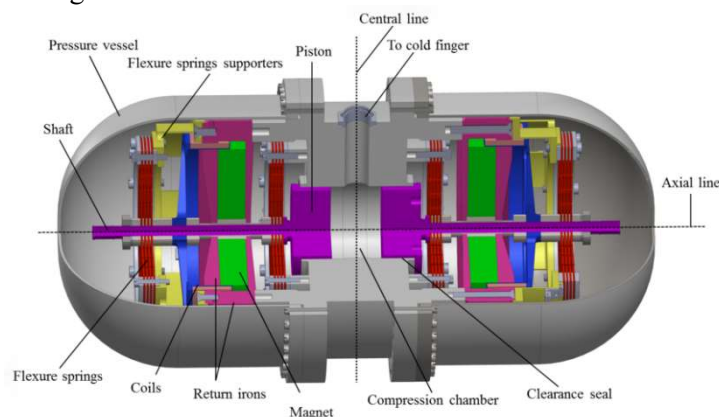


Fig.1 Structure of the developed dual-opposed moving-coil linear compressor

2.1. Force balance of the motor

According to the balance of electric potential, relation between the current, voltage, and piston displacement in the moving-coil linear compressor can be written as [7]:

$$u(t) = L_e \frac{di(t)}{dt} + R_e i(t) + BL \frac{dx}{dt} \quad (1)$$

During the operation, the force balance of the moving mass can be summarized as shown in Fig.2 and Eq.(2). It includes six dynamic forces: the linear motor force F_m , mechanical spring force F_x , gas force on the back side of the piston F_{bg} and that on the front side F_g , viscous dissipation force F_d and inertial force F_i . θ is the phase angle between the motor force and displacement. If the value of θ equals $\pi/2$, the compressor will operate at resonant state and Joule loss of the moving coil will be minimized.

$$L\dot{B}i(t) = m \frac{d^2x(t)}{dt^2} + b \frac{dx(t)}{dt} + k_x x(t) + p(t)A_p - p_B(t)A_p \tag{2}$$

↓
 F_m

↓
 F_i

↓
 F_d

↓
 F_x

↓
 F_g

↓
 F_{bg}

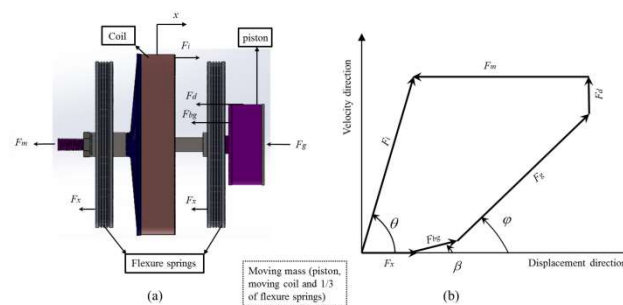


Fig.2 (a) The forces on moving components. (b) Force balance for the motor.

2.2. Magnetic circuit

The geometry of the air gap in the magnet circuit is estimated and designed. As it is shown in Fig.3, the permanent magnet is magnetized in the axial direction and long coil is adopted in the motor. The air gap is located between the two return irons with an annular shape. In consideration of the probability of intermittent contact and wear between the moving coil and return irons, the width of the air gap will be a little larger than that of the moving coil and it will be chosen according to experimental experience.

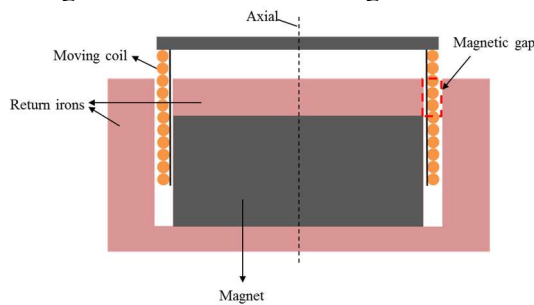


Fig. 3 Geometry of the magnet circuit.

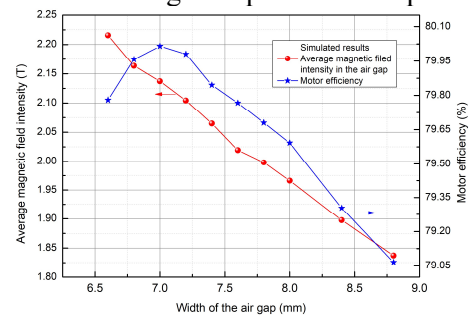


Fig.4 Simulated results of magnetic field intensity and motor efficiency under various width of air gap

Theoretically, the width of air gap should be as small as possible to maximize the average magnetic field intensity in order to obtain large motor force and high motor efficiency. Meanwhile, the effective coil volume in the air gap will be reduced correspondingly, which is unfavourable for gaining high motor force and efficiency. There should be a compromise between magnetic field intensity and effective coil volume to obtain optimal geometry of the air gap. An example of magnet circuit with a two-dimensional model will be given to explain the above circumstance in a detailed way. The impedance of cold finger is assumed and fixed. Fig.4 shows simulated results of average magnetic field intensity and motor efficiency under various widths of air gap. It is found that the average magnetic field intensity decreases monotonously with the width of air gap, while there exists an optimal width of air gap for the compressor to achieve the highest motor efficiency. These results also verify the above-mentioned analyses.

2.3. Mechanical resonance

Generally, without any load, the compressor can be regarded as a mass-spring system, and its mechanical resonant frequency will be the best operating frequency. Once the cold finger is connected, the dynamic pressure at the piston surface provides periodic gas forces on the piston surface. The gas forces can be divided into two parts, one of which is out of phase with the piston displacement and does work on the gas, like a gas damp, transporting PV power to the cold finger to achieve cooling procedure, the other one is in phase with the displacement, consuming no work, acting as a gas spring and forming a new mass-spring system.

Then, the stiffness of the gas spring and resonant frequency can be respectively defined as:

$$k_{gas} = (p(t) - p_B(t))A_p \cos \alpha / X \quad (3)$$

$$f_{mg} = \frac{1}{2\pi} \left(\frac{k_x + (p(t) - p_B(t))A_p \cos \alpha / X}{m} \right)^{1/2} \quad (4)$$

During the design of the compressor, in order to achieve high performance of the linear motor, the designed working frequency will be approximate to the resonant frequency according to the previously proposed method [8].

3. Experimental performance characteristics

According to the previous design and experience of flexure springs applied in small-scale cryocoolers, three Archimedes spirals which act as slots and the material of austenitic stainless steel are used in the design and fabrication of the flexure spring. The key parameters are listed in Table 1. Each half of the compressor employs 10 pieces of flexure spring and the total axial stiffness of the mechanical springs reaches 62 kN/m.

Then, the linear compressor is assembled and a photograph with pressure vessels uncovered is shown in Fig.5. Besides, the main parameters of each motor are tested and the results are summarized as Table 2. The moving mass includes the weight of the whole piston shaft and 1/3 weight of the flexure springs. In addition, the mechanical damp coefficient with free piston is also estimated according to the experimental results of the attenuated piston displacement.



Fig. 5 A photograph of developed compressor.

Table 1. Key parameters of the developed flexure spring

Parameters	Values
Outer diameter	200 mm
Inner diameter	15.5 mm
Slot width	2 mm
Thickness	2 mm
Axial stiffness (each piece)	6.2 kN/m

Table 2. Parameters of each motor of the developed dual-opposed linear compressor

Parameters	Values
Magnetic field intensity(B)	0.96 T
Effective coil length (L)	26 m
Coil resistance(R_e)	0.54 Ω
Clearance gap thickness	18 μm
Moving mass(m)	2.8 kg
Axial stiffness (k_x)	62 kN/m
Mechanical damp(b)	17.8 N·s/m
Piston diameter(D_p)	100 mm
Full stroke($s/2$)	11 mm

With no cold finger, variations of the power factor to the frequency under different input voltages are tested and results are shown in Fig.6. The power factor grows up gradually with frequency and then drops a little at 58 Hz, which satisfies the design goal (the resonant frequency is designed at 56 Hz). In the tests, the compressor has been coupled with a coaxial SPTC which can achieve a cooling power of 580 W at 77 K for the cooling of HTS cables, with an input electric power of 12 kW, as shown in Fig.7.

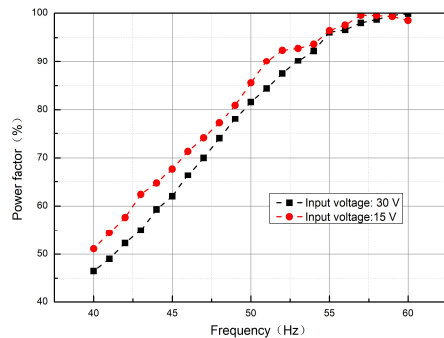


Fig.6 Relations between frequency and power factor

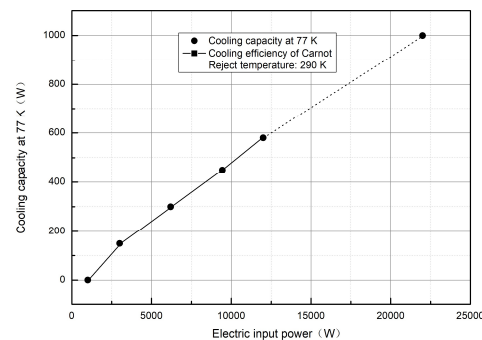


Fig.7 Cooling performance of the coupled cooler

4. Conclusions

A linearized model of a 12 kW dual-opposed moving-coil linear compressor is established in which systematic analyses about force balance, mechanical resonance and magnetic circuit are conducted. Detailed relations between the air gap and magnetic field intensity are simulated and focused on to optimize the motor efficiency, and the designs of linear motor, including the magnetic circuit, mechanical resonance, are discussed in a more detailed way. The prototype compressor is worked out and tested. The compressor has been coupled with a coaxial pulse tube cold finger, which can provide a cooling power of 580 W at 77 K with an electric input power of 12 kW.

5. Acknowledgements

The work is financially supported by The Aeronautical Science Foundation of China (No. 20162490005) and The Science and Technology Commission of Shanghai Municipality (Nos.18511110100, 18511110101 and 18511110102).

6. References

- [1] Bi, Y.F., 2013 Cooling and Cryocoolers for HTS power applications, *Applied Superconductivity and electromagnetics*, Vol. **4**, 97-108.
- [2] Lee, R.C., DaDa A., Garcia E.L. and Ringo, S.M., 2006 Performance testing of a cryogenic refrigeration system for HTS cables, *Adv Cryog Eng.* **51**, pp. 773–781.
- [3] Potratz, S.A., Abbott T.D and Johnson, M.C., 2008 Stirling-type pulse tube cryocooler with 1 kW of refrigeration at 77 K, *Adv Cryog Eng.*, **53**, pp. 42–48.
- [4] Chen, R.L., Henzler, G.W. and Royal, J.H., 2010 Reliability test of a 1-kW pulse tube cryocooler for HTS cable application, *Adv Cryog Eng.*, **55**, pp. 727-735.
- [5] Dang, H.Z., 2015 Development of high performance moving-coil linear compressors for space Stirling-type pulse tube cryocoolers, *Cryogenics*. **68**, pp. 1–18.
- [6] Ross, Jr. R.G., 2007 Aerospace coolers: a 50-year quest for long life cryogenic cooling in space, In: Timmerhaus KD, Reed RP, editors. *Cryogenic engineering: fifty years of progress*. Springer, New York, pp. 225–284.
- [7] Marquardt, E., Radebaugh, R., Kittel, P., 1993 Design equations and scaling laws for linear compressors with flexure springs, *Cryocoolers* **7**, pp.783–804.
- [8] Dang, H.Z., Tan, J., Zhang, L., 2016 Theoretical and experimental investigations on the optimal match between compressor and cold finger of the Stirling-type pulse tube cryocooler, *Cryogenics* **76**, pp.33-46.